Subchoroidal Release of VEGF and bFGF Produces Choroidal Neovascularization in Rabbit

Article *in* Current Eye Research · October 2016

DOI: 10.1080/02713683.2016.1227448

CITATIONS
18

READS
216

7 authors, including:

Corinne Wong
SCLERA LLC United States
24 PUBLICATIONS **398** CITATIONS
SEE PROFILE

Kathryn Osann
University of California, Irvine
345 PUBLICATIONS **13,814** CITATIONS
SEE PROFILE

Fred N. Ross-Cisneros
Doheny Eye Institute
82 PUBLICATIONS **4,753** CITATIONS
SEE PROFILE

Grit Zahn
Eternygen
52 PUBLICATIONS **2,005** CITATIONS
SEE PROFILE

Current Eye Research

ISSN: 0271-3683 (Print) 1460-2202 (Online) Journal homepage: http://www.tandfonline.com/loi/icey20

Subchoroidal Release of VEGF and bFGF Produces Choroidal Neovascularization in Rabbit

Corinne G. Wong, Mehran Taban, Kathryn Osann, Fred N. Ross-Cisneros, T. C. Bruice, Grit Zahn & Timothy You

To cite this article: Corinne G. Wong, Mehran Taban, Kathryn Osann, Fred N. Ross-Cisneros, T. C. Bruice, Grit Zahn & Timothy You (2016): Subchoroidal Release of VEGF and bFGF Produces Choroidal Neovascularization in Rabbit, Current Eye Research, DOI: 10.1080/02713683.2016.1227448

To link to this article: http://dx.doi.org/10.1080/02713683.2016.1227448

Published online: 17 Oct 2016.

CURRENT EYE RESEARCH
http://dx.doi.org/10.1080/02713683.2016.1227448

Taylor & Francis
Taylor & Francis Group

Subchoroidal Release of VEGF and bFGF Produces Choroidal Neovascularization in Rabbit

Corinne G. Wong[a], Mehran Taban[b], Kathryn Osann[c], Fred N. Ross-Cisneros[d], T. C. Bruice[e], Grit Zahn[f], and Timothy You[g]

[a]SCLERA LLC, Carlsbad, CA, USA; [b]Department of Ophthalmology, College of Medicine, University of California Irvine, Irvine, CA, USA; [c]Department of Medicine, College of Medicine, University of California Irvine, Irvine, CA, USA; [d]Doheny Eye Institute, Los Angeles, CA, USA; [e]University of California Los Angeles, Los Angeles, CA, USA; [f]Consulting, Berlin, Germany; [g]Orange County Retina Group, Santa Ana, CA, USA

ABSTRACT

Purpose: Intravitreal vascular endothelial growth factor (VEGF) and basic fibroblast growth factor (bFGF) produced florid retinal neovascularization and hemorrhage in the rabbit. This study seeks to determine whether sustained subchoroidal release of both VEGF and bFGF can induce robust choroidal neovascularization (CNV) in the rabbit.

Methods: Subchoroidal implantation through the sclera of polymeric pellets containing both 15 µg VEGF and 15 µg bFGF was performed on adult pigmented male Dutch belted rabbits ($N = 6$) and NZW albinos ($N = 8$). As negative controls, blank pellets with no growth factors were implanted in both Dutch belted rabbits ($N = 6$) and NZW albino rabbits ($N = 4$). Development of CNV was documented weekly over a 4-week period with indirect ophthalmoscopy, color fundus photography, and fluorescein angiography. Eyes were enucleated and prepared for histologic and immunohistochemical analyses at the end of the study. Amounts of VEGF and bFGF that were released *in vitro* from the pellets were measured by ELISA.

Results: In all eyes with subchoroidal implants containing both VEGF and bFGF, strong fluorescein leakage was observed at 2, 3, and 4 weeks ($P < 0.005$); no leakage was seen initially in week 1. Negative control groups with blank implants showed no fluorescein leakage throughout the 4-week study period. Histologic analysis confirmed the presence of experimental CNV. New subretinal blood vessel growth occurred in all eyes with VEGF/bFGF implants. Negative control eyes with blank implants showed no vascular changes. *In vitro* sustained release of both VEGF and bFGF was confirmed by ELISA.

Conclusion: Sustained subchoroidal release of both VEGF and bFGF produced experimental CNV rapidly in the rabbit. Understanding how these growth factors induce CNV may suggest novel therapeutic strategies in the large rabbit eye.

ARTICLE HISTORY
Received 1 February 2016
Revised 7 June 2016
Accepted 17 August 2016

KEYWORDS
Basic fibroblast growth factor; robust rabbit CNV model; subchoroidal sustained release; transscleral implantation; vascular endothelial growth factor

Introduction

Age-related macular degeneration (AMD) is the leading cause of acquired blindness and vision impairment among elderly Americans.[1] Up to 17 million elderly Americans have at least the early signs of this debilitating disease, which increases with age and affects one in six Americans between the age of 55 and 64 years.[1] Approximately 90% of patients with AMD possess the non-neovascular dry form that is characterized by atrophy of the retinal pigment epithelium (RPE) and subsequent loss of macular photoreceptors.[1,2] The wet, exudative neovascular form of AMD affects approximately 10% of those with this chronic disease and leads to severe visual loss.[2,3] The hallmark of neovascular wet AMD is choroidal neovascularization (CNV) with its abnormal growth of new blood vessels.[3–5]

To study the pathogenesis of neovascular AMD and test therapeutic treatments, a pre-clinical model of CNV needs to be developed in a large animal eye that is similar in size to the human eye. Laser-induced CNV has been produced in rodents, pigs, and monkeys.[6–9] Attempts to replicate laser-generated experimental CNV in the rabbit have been unsuccessful.[10,11] Our earlier studies showed that sustained intravitreal release of vascular endothelial growth factor (VEGF) and basic fibroblast growth factor (bFGF) in the pigmented Dutch belted rabbit initiated florid retinal NV with subsequent hemorrhage and retinal detachment.[12] Our previous studies also demonstrated that neither sustained release of VEGF nor bFGF alone produced retinal NV in the Dutch belted rabbit.[12,13] Both VEGF and bFGF have been detected in the vitreous of patients with proliferative diabetic retinopathy and in epiretinal and choroidal neovascular membranes.[14–18] Therefore, the goal of this study is to assess whether sustained-release of both VEGF and bFGF within the subchoroidal space in both NZW albino and Dutch belted rabbits can induce robust CNV.

Materials and methods

Subchoroidal implantation of sustained-release pellets

All procedures were conducted in accordance with the Association for Research in Vision and Ophthalmology Statement for the Use of Animals in Ophthalmic and Vision Research and the US Department of Agriculture Animal

CONTACT Corinne G. Wong cgwong@scleracorp.com SCLERA LLC, 6965 El Camino Real, Suite 105-502, Carlsbad, CA 92009, USA.
Color versions of one or more of the figures in the article can be found online at www.tandfonline.com/icey.

Welfare Act as well as conditions specified in the Guide for the Care and Use of Laboratory Animals. The protocol was approved by the facility institutional animal care and use committees (North American Science Associates, Inc., Irvine, CA, USA).

Adult male rabbits weighing between 2.0 and 3.0 kg were anesthetized with 35 mg/kg intramuscular injection of ketamine (Phoenix Pharmaceuticals, Inc., St. Joseph, MO, USA) and 5 mg/kg xylazine (Lloyd Laboratories, Shenandoah, IA, USA). Pupils were dilated with topical 2.5% phenylephrine (Alcon, Fort Worth, TX, USA) and 1% tropicamide (Bausch & Lomb, Tampa, FL, USA). A total of 24 animals were utilized in this study.

Sterile preparations of both human recombinant VEFG 165 and recombinant bFGF (PeproTech, Rocky Hill, NJ, USA) were incorporated into a Hydron polymer (Hydromed Sciences, Cranbury, NJ, USA) following specifications of the manufacturer. Also, phosphate-buffered solution (PBS) was incorporated into the Hydron polymer to produce blank pellets that acted as negative blank controls. Specifically, 15 μg of human recombinant VEGF and 15 μg of recombinant bFGF (PeproTech) were incorporated into each implant per manufacturer's instructions. Under a Zeiss operating microscope, a temporal conjunctival peritomy involving 3 clock hours was performed using Westcott scissors and micro-forceps. After a marker was used to measure a distance 2.5 mm posterior to the corneal limbus, a curvilinear incision was created with a Number 15 Bard-Parker blade extending from the 9:30 position with care to avoid the ciliary vasculature. A 4 mm full thickness scleral incision was performed that avoided the choroid.[19,20,21] The scleral incision was created until the underlying choroidal tissue was evident. A blunt cyclodialysis spatula was used to create a small subchoroidal pocket between the choroid and sclera for placement of the non-biodegradable Hydron pellet. The pellet was held with a non-toothed forceps and guided as posteriorly as possible between the 9 o'clock and 10 o'clock position to rest in the subchoroidal space. The scleral incision was closed with an interrupted 7-0 vicryl suture. The overlying conjunctival peritomy was re-approximated and closed with 7-0 vicryl sutures. Indirect ophthalmoscopy was performed to confirm proper placement of the pellet and confirm the lack of complications. Povidone iodine, a topical antibiotic ointment that is used for asepsis, was placed on the rabbit eye. After the 10-minute procedure, each rabbit was transferred to a recuperation room for recovery from the surgical operation and anesthesia. A total of 24 animals were utilized in this study. Fourteen animals (N = 6 for Dutch belted and N = 8 for NZW albinos) were implanted with the VEGF/bFGF pellet. Ten animals acting as negative controls (N = 6 for pigmented Dutch belted and N = 4 for NZW albino rabbits) were implanted with blank pellets that contained no growth factors. Contralateral eyes were not used in any animal. Animals were examined by indirect ophthalmoscopy before and immediately after surgery, 48 hours, 4 days, and weekly over a 28-day period. Finally, all animals were euthanized at the end of the study with an intravenous injection of sodium pentobarbital veterinary solution (JA Webster, Inc., Sterling, MA, USA). Right eyes from all animals were enucleated for histological analysis. Contralateral eyes were not utilized since right eyes with blank implants were used as negative controls.

Color fundus photography and fluorescein angiography

Color fundus photography and fluorescein angiography (FA) were performed pre-operatively and on a weekly basis after subchoroidal pellet implantation for four consecutive weeks with a TOPCON retinal digital camera system (Topcon Medical Systems, Oakland, NJ, USA). Fluorescein sodium (10% solution) was administered intravenously through the right ear vein of the anesthetized rabbit. Photographs were taken during a 30-second period for up to 10 minutes. Digital photographic files were stored in the TOPCON ImageNET software program. The digitized photographs were evaluated independently by two observers in a masked fashion. Evaluations were performed visually. There was 100% agreement between the two observers who did not perform the surgical implants.

Fls (FAs) of the rabbit CNV were graded on a scale from 0, 1, 2, and 3. Grade 0 – no leakage at early and late fluorescein angiographic phases; Grade 1 – mild leakage at both early and late fluorescein angiographic phases with a mild degree of fluorescence without uniform fluorescence in the late frames; Grade 2 – moderate leakage at early and late fluorescein angiographic phases with a moderate degree of fluorescence, which covers 50% or more of the lesion in the late frames; Grade 3 – marked leakage at both early and late fluorescein angiographic phases with severe degree of fluorescence that is characterized by significant leakage in the early phases, which persist throughout the transit and late frames. Statistical analysis for the severity of fluorescein leakage over time on a scale of 0–3 was performed utilizing the Kruskal–Wallis non-parametric test.

Histology

For histological analysis, the implanted right eyes were enucleated, corneas were removed, and the whole eyes were immersion-fixed in 10% phosphate-buffered formalin for a minimum of 24 hours. The eyes then were rinsed in phosphate buffer; both the iris and lens were excised. The posterior segments of the eyes were excised from the anterior segments. Next, a complete para-sagittal cut was made 90° to the horizontal plane and medial to the implant with the optic disk as a reference. FAs were used to orient the cutting position close to the site of the implant. Eyes then were processed for paraffin embedding by dehydration in progressively higher concentrations of ethanol–water, cleared with Histoclear (National Diagnostics, Manville, NJ, USA), and infiltrated with paraffin in a Fisher Model 166 MP tissue processor. After the samples were embedded in paraffin, the tissue margins were oriented carefully so that the pellet implantation site was flush with the face of the paraffin tissue block. Then 4 μm serial cross-sections were cut on a paraffin retracting microtome. The sections were placed on albumin-coated glass slides, de-paraffinized with Histoclear, stained with hematoxylin and eosin (H&E), and cover-slipped. Once the beginning

of the implant site was determined, that slide was labeled as 1 in the subsequent sequences of tissue sections. Generally, the first slide and every tenth slide were stained with H&E for histological evaluations. Serial sections of 10 slides were examined.

Immunohistochemistry

Microscopic slides with tissue sections were de-paraffinized and then hydrated in distilled water. The standard antigen retrieval procedure was performed. Slides were placed in a commercially available buffer at pH 9.5 and heated in a self-contained steamer with a microwave oven. After a cooling period, the slides were washed, blocked for endogenous peroxidase, and subsequently labeled with a mouse monoclonal antibody directed against type IV collagen (mouse monoclonal anti-human collagen IV; clone CIV 22; Dako Cytomation, Inc., Carpinteria, CA, USA). Using an indirect method, slides subsequently were treated with biotinylated-horse-anti-mouse antibody (B-2000, Vector Laboratories, Burlingame, CA, USA), then developed by incubation with the avidin-biotinylated complex (ABC kit Vectastain PK-6100, Vector Laboratories), and finally followed by reaction with diaminobenzidine (DAB) and hydrogen peroxide as the substrate-chromagen to produce a brownish black stain (SK-4100, Vector Laboratories) for visualization. All slides subsequently were counter-stained with hematoxylin (Fisher CS401-D, Vector Laboratories), dehydrated, soaked in xylene, and mounted with Permount (Fisher SP15-100, Vector Laboratories). The appropriate samples were evaluated at the light microscopic level after staining; and the histologic images were acquired with an Olympus BHT2 photomicroscope that is coupled to a Spot II digital camera (Diagnostic Instruments, Inc., Sterling Heights, MI, USA).

Enzyme-linked immunosorbent assay

Enzyme-linked immunosorbent assay (ELISA) was utilized to confirm amounts of VEGF and bFGF (PeproTech) that were released over 7 days from the VEGF/bFGF implants under in vitro conditions (human VEGF and bFGF Quantikine ELISA kits, R&D Systems, Minneapolis, MN, USA). The stability of both VEGF and bFGF was guaranteed for up to 1 week by the manufacturer when these lyophilized recombinant proteins were reconstituted as directed and then diluted further into phosphate-buffered saline (PBS). Assays with serially diluted standards were performed in triplicate and repeated on three independent occasions in accordance with the manufacturer's instructions. A total of 18 VEGF/bFGF-containing implants were used. Means ± SEM were plotted on Microsoft EXCEL (Microsoft Corporation, San Diego, CA, USA).

Results

All animals were documented as having healthy retinas by indirect ophthalmoscopy, fundus photography, and FAs prior to implantation of VEGF/bFGF-containing pellets. Retinal detachments were not detected prior to the onset of experimental CNV. At 48 hours, transitory localized inflammatory response was seen visually by indirect ophthalmoscopy at the implantation site in all eyes, which receded by day 4. These initial changes most likely were due to the implantation procedures.

At the end of the 4-week period, subretinal hemorrhages, exudates, and pigment dispersion with atrophy of the RPE appeared in eyes with VEGF/bFGF-containing implants but not in eyes with blank implants. In eyes with VEGF/bFGF-containing implants, color fundus photographs in the first week demonstrated localized elevation at the site of the pellet placement (Figure 1). The location was along the distal edge of the optic streak either at the temporal raphe or immediately superior to the myelinated optic streak. Fluorescein leakage was not seen in week 1, while robust fluorescein leakage was seen at week 2 and continued through both week 3 and week 4 ($P < 0.005$), as shown in Figure 1 for NZW albinos and Figure 2 for pigmented Dutch belted rabbits. In the negative control groups with blank implants, fluorescein leakage was not seen during the 4-week study period as shown in Figure 3. Additionally, both histologic assessment and immunohistochemical analysis at the end of the 4-week study confirmed the presence and localization of experimental CNV in eyes with VEGF/bFGF-containing implants. Light micrographs at 28 days after implantation of VEGF/bFGF-containing pellets are shown in Figure 4, left, which demonstrated experimental CNV via red blood cell (RBC) observations. Experimental CNV penetrated Bruch's membrane with phagocytosis of RBCs by the RPE from the basal side. Melanin granules of the RPE cells were transferred from the basal to apical side (Figure 4, right). Small spherical "pieces" of RBCs that are endocytosed by the RPE cells appear to be located within the cytoplasm of the RPE cells. Results with immunohistochemical staining for type IV collagen showed that Bruch's membrane stained positively in animals with experimental CNV and that the CNV occurred anterior to Bruch's membrane (Figure 5). Finally, in vitro ELISA studies showed the levels of both VEGF and bFGF over a 7-day period (mean ± SEM) as described in Figure 6. VEGF levels peaked at day 5; and bFGF levels appeared to peak by day 7.

Discussion

This study demonstrates that sustained release of both VEGF and bFGF within the subchoroidal space produced experimental CNV in both NZW albino and pigmented Dutch belted rabbits. These animals developed severe fluorescein leakage and histological alterations that were consistent with CNV. In vitro ELISA studies confirmed the sustained release of both VEGF and bFGF over a 7-day period. Approximately 95% of the animals developed experimental CNV. Neovascularization typically occurred after 7 days postoperatively when the effects of surgical trauma waned. Subchoroidal release of both angiogenic factors VEGF and bFGF provided the necessary induction of abnormal blood vessel growth that lead to experimental CNV. The time course and robustness were similar between NZW albinos and Dutch belted rabbits. Lack of pigmentation in the albino rabbit allowed for observation of both the choroidal vasculature and its patterns during the time course of experimental CNV. FA analysis confirmed significant vascular leakage that occurred after the

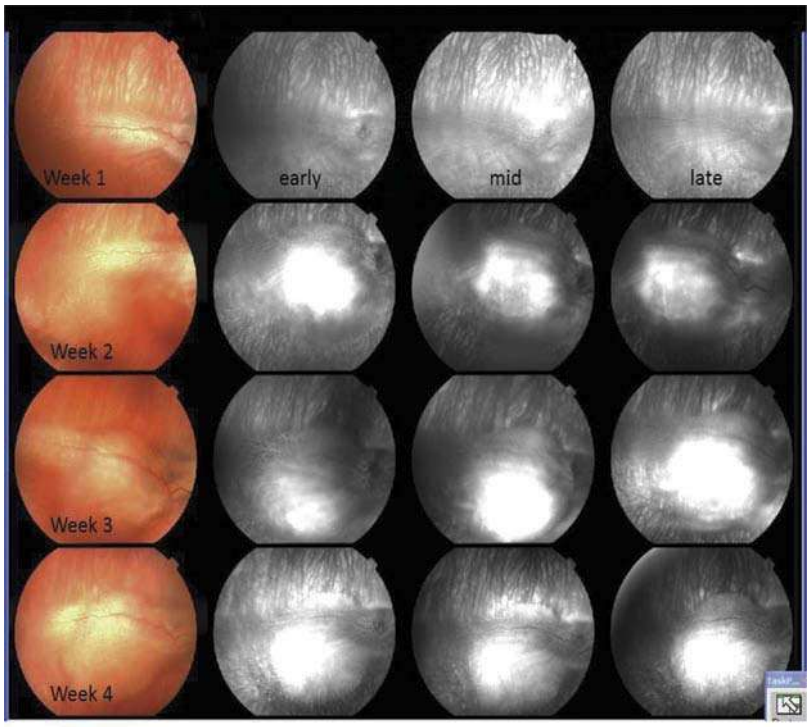

Figure 1. In the NZW albino rabbit, color fundus photographs showed results of subchoroidal implantation of the VEGF/bFGF pellet. Early, mid-, and late phases of the FAs are shown from left to right. FAs at weeks 1, 2, 3, and 4 demonstrated the progression of experimental CNV with no fluorescein leakage detected in week 1. At week 1, experimental CNV was graded at Grade 0. At week 2, experimental CNV was graded at Grade 2. At both weeks 3 and 4, the maximum Grade 3 occurred for all animals.

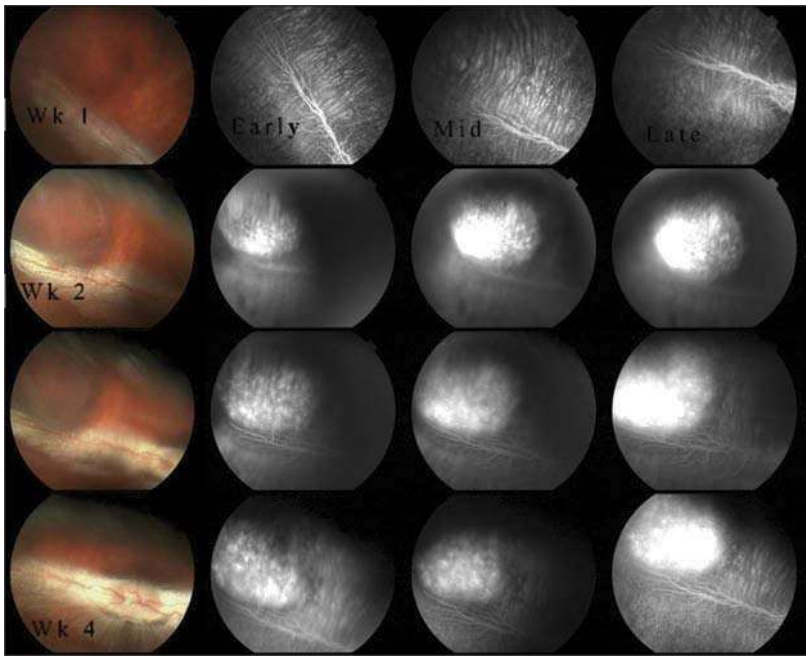

Figure 2. Color fundus photographs displayed the VEGF/bFGF-containing implant in the subchoroidal space of the pigmented Dutch belt rabbit. FAs at week 1 displayed no fluorescein leakage. At weeks 2, 3, and 4, fluorescein leakage (early, mid-, and late phases) can be seen (left to right) with Grade 3 for these time points.

first week and became greater in the following weeks. Presumably, both VEGF and bFGF within the implanted pellets were depleted within the 4-week study period. In vitro ELISA studies confirmed the sustained release of both VEGF and bFGF from the implants.

In addition, both histologic and immunohistochemical analysis at the light microscopic level confirmed experimental CNV. Interestingly, changes in the RPE during experimental CNV included melanin re-distribution from the basal to the apical side and potentially may indicate a mechanism by the

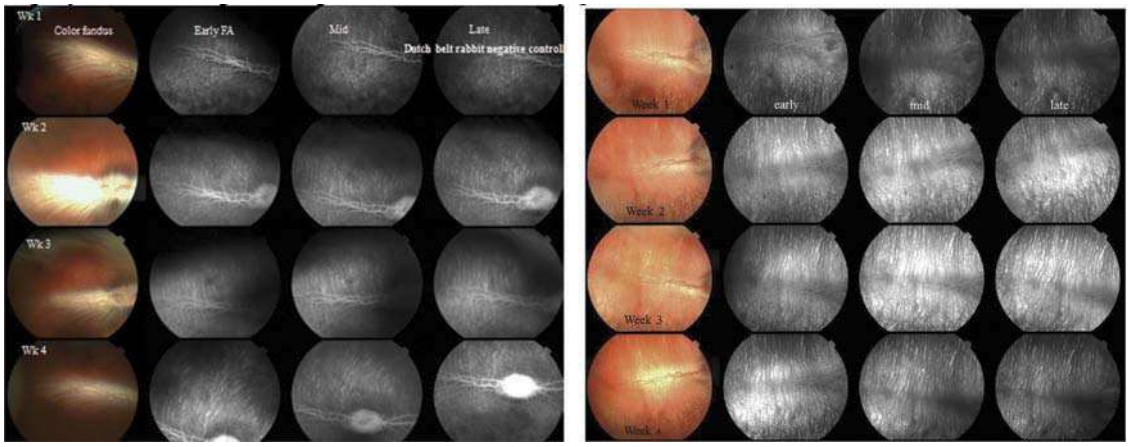

Figure 3. (Left) FAs of a negative control Dutch belt rabbit demonstrate that the blank implant at weeks 1, 2, 3, and 4 showed no leakage during the 4-week study period (left to right: early, mid-, and late phases). (Right) Negative control NZW albinos also displayed no leakage during the 4-week study period.

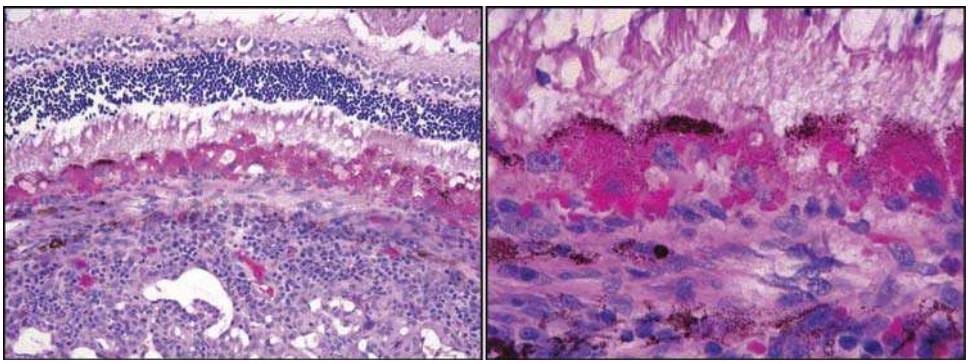

Figure 4. (Left and Right) In a pigmented Dutch belted rabbit, experimental CNV penetrated Bruch's membrane with phagocytosis of red blood cells (RBCs) by the RPE from the basal side. Most RPE cells have become distended from engulfing numerous RBCs, which are located within the cytoplasm of the RPE cells. Melanin granules of the RPE cells have been transferred from the basal to the apical side (50×).

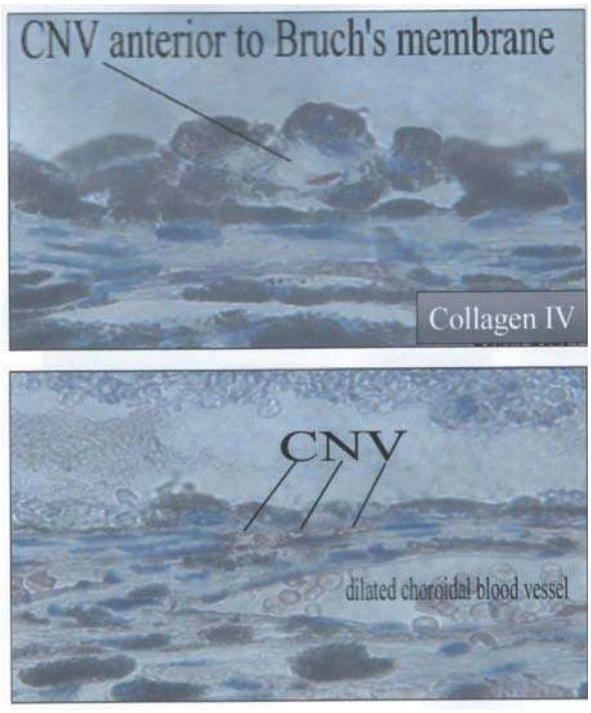

Figure 5. Immunohistochemical staining for type IV collagen showed the presence of both abnormal dilated blood vessels and experimental CNV anterior to Bruch's membrane (50×).

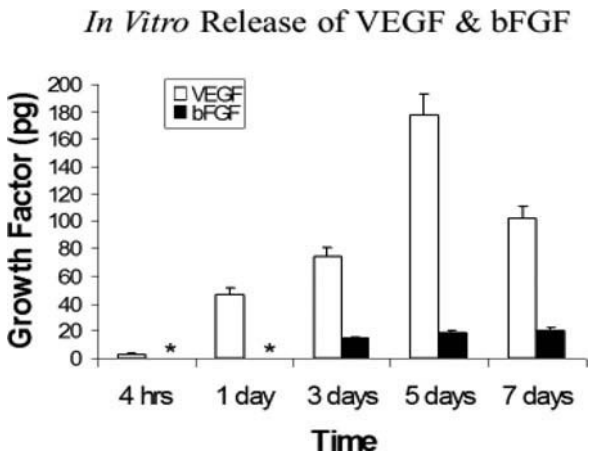

Figure 6. ELISA was used to determine the amounts of VEGF and bFGF that were released from the Hydron implant under in vitro conditions (N = 18). VEGF levels peaked at day 5 and bFGF levels peaked at day 7 (mean ± SEM).

RPE to diminish chronic oxidative stress. Type IV collagen immunostaining was demonstrated in the rabbit Bruch's membrane after development of CNV. In aged eyes, 2CD-31 immunostaining, which demonstrates the presence of endothelial cells, also showed strong positive staining in this

experimental rabbit CNV model (results not shown). Further studies will define how such early changes at the RPE/Bruch's membrane interface may relate to the early initiation of CNV.

Moreover, our earlier studies demonstrated that eyes with bFGF-containing pellets in the vitreous displayed no retinal vascular changes while eyes with high levels of VEGF-containing pellets showed mild vascular changes.[12] Since b-FGF contributes to angiogenesis by inducing VEGF expression in endothelial cells of forming capillaries,[23] combination of both VEGF and bFGF in these implants provided the necessary induction of CNV in the rabbit eye. Other experimental CNV models have been described in rabbits.[24–26] However, neither bFGF nor VEGF in subretinal injections through the vitreous produced a reliable CNV model in the rabbit; and one study showed that Matrigel alone induced CNV.[26] Also, our experimental rabbit CNV model compared favorably with the laser-induced cynomolgus monkey CNV model in another study.[27]

In conclusion, pathological changes leading to neovascular AMD occur within the choriocapillaris, Bruch's membrane, and the RPE. Subchoroidal delivery of angiogenic growth factors that successfully initiated experimental CNV more likely resembles the clinical condition leading to neovascular AMD. Currently, both barrier and permeability limitations continue to thwart therapeutic interventions for chorioretinal diseases. Research on subchoroidal delivery of potential therapeutics with biocompatible implant materials is ongoing. Use of subchoroidal micro-devices for delivery of therapeutics can decrease dosing frequency in a potentially minimally invasive procedure and may reduce side effects. Initial pathologic changes within Bruch's membrane and the RPE may be initiated by chronic oxidative stress[34] and inflammatory processes that subsequently lead to CNV.[35,36] Such early changes can be studied in this experimental rabbit CNV model and may yield early clues on the pathogenesis of CNV. Ultimately, understanding the intricate molecular interplay of various angiogenic and anti-angiogenic factors and their respective receptors will provide further understanding on the development of new abnormal vascular beds beneath the retina. Such studies presumably will lead to the design of novel therapeutics for treatment of retinal-related neovascular diseases.

Declaration of interest

The authors report no conflicts of interest. The authors alone are responsible for the content and writing of the paper.

References

1. National Eye Institute. Available at http://www.nei.nih.gov/.
2. Abselsalam, A, Del Priore L, Zarbin MA. Drusen in age-related macular degeneration: pathogenesis, natural course, and laser photocoagulation-induced regression. Surv Ophthalmol 1999;44:1–29.
3. Rattner A, Nathans J. Macular degeneration: recent advances and therapeutic opportunities. Nat Rev Neurosci 2006;7:860–872.
4. Crabb JW, Miyagi M, Gu X, Shadrach K, West KA, Sakaguchi H, et al. Drusen proteome analysis: an approach to the etiology of age-related macular degeneration. Proc Natl Acad Sci USA 2002;99:14682–14687.
5. Ambati J, Ambati BK, Yoo SH, Ianchulev S, Adamis AP. Age-related macular degeneration: etiology, pathogenesis, and therapeutic strategies. Surv Ophthal 2003;48:257–293.
6. Ryan SJ. Subretinal neovascularization: natural history of an experimental model. Arch Ophthal 1982;100:1804–1809.
7. Miller H, Miller B, Ryan SJ. The role of retinal pigment epithelium in the involution of subretinal neovascularization. Invest Ophthalmol Vis Sci 1986;27:1644–1652.
8. Frank RN, Das A, Weber ML. A model of subretinal neovascularization in the pigmented rat. Curr Eye Res 1989;8:239–247.
9. Kiilgaard JF, Andersen MVN, Wiencke AK, Scherfig E, La Cour M, Tezel TH, et al. A new animal model of choroidal neovascularization. Acta Ophthalmol Scandinavica 2005;83:697–704.
10. Hsu HT, Goodnight R, Ryan SJ. Subretinal choroidal neovascularization as a response to penetrating retinal injury in the pigmented rabbit. Jpn J Ophthalmol 1989;33:358–366.
11. El Dirini AA, Ogden TE, Ryan SJ. Subretinal endophotocoagulation: a new model of subretinal neovascularization in the rabbit. Retina 1991;11:244–249.
12. Wong CG, Rich KA, Liaw LHL, Hsu HT, Berns MW. Intravitreal VEGF and bFGF produce florid retinal neovascularization and hemorrhage in the rabbit. Curr Eye Res 2001;22:140–147.
13. Erb MH, Sioulis CE, Kuppermann BD, Osann K, Wong CG. Differential retinal angiogenic response to sustained intravitreal release of VEGF and bFGF in different pigmented rabbit breeds. Curr Eye Res 2002;24:245–252.
14. Adamis AP, Miller JW, Bernal MT, D'Amico DJ, Folkman J, Yeo TK, et al. Increased vascular endothelial growth factor levels in the vitreous of eyes with proliferative diabetic retinopathy. Am J Ophthalmol 1994;118:445–450.
15. Aiello LP, Avert RL, Arrigg PG, Keyt BA, Jampel HD, Shah ST, et al. Vascular endothelial growth factor in ocular fluid of patients with diabetic retinopathy and other retinal disorders. N Engl J Med 1994;331:1480–1487.
16. Sivalingam A, Kinney J, Brown GC, Benson WE, Donoso L. Basic fibroblast growth factor levels in the vitreous of patients with proliferative diabetic retiopathy. Arch Ophthalmol 1990;108:869–872.
17. Frank RN, Amin RH, Eliott D, Puklin JE, Abrams GW. Basic fibroblast growth factor and vascular endothelilial growth factor are present in epiretinal and choroidal neovascular membranes. Am J Ophthalmol 1996;122:393–403.
18. Yancopoulos GD, Davis S, Gale NW, Rudge JS, Wiegand SJ, Holash J. Vascular-specific growth factors and blood vessel formation. Nature 2000;407:242–248.
19. Wong CG, Gum GG, Hagemann L, Marques L, Kuppermann BD, de Carvalho RP. Induction of choroidal neovascularization by sustained release of VEGF/bFGF in rabbits: angiographic characterization and histologic correlation on different patterns of the choroidal vascular response. Invest Ophthalmol Vis Sci 2005;46e-abstract 1417.
20. Wong CG, Bruice TC, You TT. Experimental CNV after transscleral implantation of VEGF/bFGF-implant within the suprachoroidal space for defining potential long-term synergistic actions of ranibizumab (Lucentis) with small low cost molecules in ameliorating wet AMD. Invest Ophthalmol Vis Sci 2008;49e-abstract 1372.
21. Rabin D, Bruice TC, You TT, Wong CG. Both edema and leakage are expressed and are separable in long-term experimental CNV via sustained simultaneous release of VEGF and bFGF within the suprachoroidal space through trans-scleral implantation of a delivery device. Invest Ophthalmol Vis Sci 2008;49e-abstract 1374.
22. Chen L, Miyamura N, Ninomiya Y, Handa JT. Distribution of the collagen IV isoforms in human Bruch's membrane. Br J Ophthalmol 2003;87:212–215.;83:141–152.
23. Seghezzi G, Patel S, Ren CJ, Gualandris A, Pintucci G, Robbins ES, et al. Fibroblast growth factor-2 (FGF-2) induces vascular endothelial growth factor (VEGF) expression in the endothelial cells of forming capillaries: an autocrine mechanism contributing to angiogenesis. J Cell Biol 1998;141:1659–1673.
24. Sylvie J, Kreppel F, Beck S, Heiduschka P, Brito V, Schnichels S, et al. A reproducible and quantifiable model of choroidal neovascularization

induced by VEGF A165 after subretinal adenoviral gene transfer in the rabbit. Molecular Vis 2008;14:1358–1372.
25. Ni M, Holland M, Jarstadmarken H, DeVries G. Time-course of experimental choroidal neovascularization in Dutch-Belted rabbit: clinical and histological evaluation. Exp Eye Res 2005;8:286–297.
26. Qiu G, Stewart JM, Sadda S, Freda R, Lee S, Guven D, et al. A new model of experimental subretinal neovascularization in the rabbit. Exp Eye Res 2006;83:141–152.
27. Zahn G, Vossmeyer D, Stragies R, Wills M, Wong CG, Löffler KU, et al. Pre-clinical evaluation of the novel small-molecule integrin α5β1 inhibitor JSM6427 in monkey and rabbit models of choroidal neovascularization. Arch Ophthalmol 2009;127:1329–1335.
28. Geroski DH, Edelhauser HF. Transscleral drug delivery for posterior segment disease. Adv Drug Deliv Rev 2001;52:37–48.
29. Kim SH, Lutz RJ, Wang NS, Robinson MR. Transport barriers in transscleral drug delivery for retinal diseases. Ophthalmic Res 2007;39:244–254.
30. Barocas VH, Balachandran RK. Sustained transscleral drug delivery. Expert Opin Drug Deliv 2008;5:1–10.
31. Pearce W, Hsu J, Yeh S. Advances in drug delivery to the posterior segment. Curr Opin Ophthalmol 2015;26:233–239.
32. Patel RS, Lin ASP, Edelhauser HF, Rausnitz MR. Suprachoroidal drug delivery to the back of the eye using hollow microneedles. Pharm Res 2011;28:166–176.
33. Lambrou FH, Chilbert M, Mieler WF, Williams GA, Olsen KA. New technique for subchoroidal implantation of experimental malignant melanoma. Invest Ophthal Vis Sci 1988;29:995–998.
34. Rabin DL, Rabin RL, Blenkinsop TA, Temple S, Stern JH. Chronic oxidative stress upregulates drusen-related protein expression in adult human RPE stem cell-derived RPE cells: A novel culture model for dry AMD. Aging 2013;5:51–66.
35. Ambati J, Atkinson JP, Gelfand BD. Immunology of age-related macular degeneration. Nat Rev Immunol 2013;13:438–451.
36. Bhutto I, Lutty G. Understanding age-related macular degeneration (AMD): relationships between the photoreceptor/retinal pigment epithelium/Bruch's membrane/choriocapillaris complex. Mol Aspects Med 2012;33:295–317.